Neural Network Security: Hiding CNN Parameters with Guided Grad-CAM

Linda Guiga[1,*] and A. W. Roscoe[2]
[1]*IDEMIA and Télécom ParisTech, Paris, France*
[2]*Department of Computer Science, University of Oxford, Oxford, U.K.*

Keywords: CNN, Security, Reverse-engineering, Grad-CAM, Parameter Protection.

Abstract: Nowadays, machine learning is prominent in most research fields. Neural Networks (NNs) are considered to be the most efficient and popular architecture nowadays. Among NNs, Convolutional Neural Networks (CNNs) are the most popular algorithms for image processing and image recognition. They are therefore widely used in the industry, for instance for facial recognition software. However, they are targeted by several reverse-engineering attacks on embedded systems. These attacks can potentially find the architecture and parameters of the trained neural networks, which might be considered Intellectual Property (IP). This paper introduces a method to protect a CNN's parameters against one of these attacks (Tramèr et al., 2016). For this, the victim model's first step consists in adding noise to the input image so as to prevent the attacker from correctly reverse-engineering the weights

1 INTRODUCTION

Deep learning is ever more important, touching most research areas. Among deep learning models, Convolutional Neural Networks (CNNs) are often used when it comes to image processing and classification (Krizhevsky et al., 2012; Coskun et al., 2017). For this reason, CNNs can be found on many embedded systems from our daily lives - such as smartphones. Face ID, the face recognition feature on the IPhone X, is an example (Inc., 2017).

Because of the efficiency of CNNs in image classification and processing, industry makes much use of them. This entails two security problems: it is necessary to protect the companies' intellectual property (IP) and to ensure the output has not been tampered with. Indeed, since finding the optimal architecture and parameters for a CNN require much time and computational power, the model used is part of the company's IP and should be kept safe from potential malicious competitors. Second, for some applications - such as face recognition - it must be infeasible to find an input on which the output is incorrect. Learning the parameters of the embedded CNN can turn such a problem from infeasible to feasible.

In the case of face recognition, for instance, an attacker who can manipulate the output of a model could impersonate someone and steal, for instance, the data on a mobile phone (Sharif et al., 2016; Deb et al., 2019; Dong et al., 2019).

Unfortunately, CNNs are the target to many different attacks. The most common attacks are *adversarial* ones. The goal of an *adversarial attack* is to change the model's output for some selected inputs, without changing the predictions for the other inputs. This is the basis of the impersonation attacks in (Dong et al., 2019). Since adversarial attacks are made easier if the attacker knows the model's parameters and architecture (Akhtar and Mian, 2018), protecting them is paramount.

However, multiple reverse-engineering attacks can potentially extract the victim model's key parameters (Tramèr et al., 2016; Oh et al., 2018).

In that context, this paper aims at protecting CNNs against equation-solving reverse-engineering attacks (Tramèr et al., 2016) by adding noise to the input, using visualization maps. Its main contribution is the use of random noise as a way of protecting the parameters against reverse-engineering attacks - rather than protecting the input data or increasing accuracy.

The first section of this paper describes the necessary background for the method. In the second section, we detail our proposed method. In the last section, we explain our experiments and show the effi-

[*] Work conducted at the University of Oxford.

Guiga, L. and Roscoe, A.
Neural Network Security: Hiding CNN Parameters with Guided Grad-CAM.
DOI: 10.5220/0009061206110618
In *Proceedings of the 6th International Conference on Information Systems Security and Privacy (ICISSP 2020)*, pages 611-618
ISBN: 978-989-758-399-5; ISSN: 2184-4356

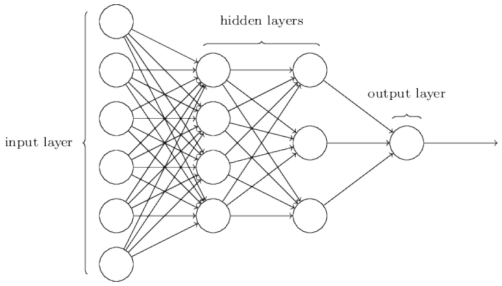

Fig. 2: Multi layer perceptron.

Figure 1: Multi Layer Perceptron (Image taken from (Batina et al., 2019)).

ciency of our method against Tramèr et al.'s equation-solving attack.

2 BACKGROUND AND RELATED WORK

In this section, we describe neural networks, detail an attack on the parameters of a neural network and explain Guided Grad-CAM, a visualization mapping we will use in our defence.

2.1 Neural Networks

A neural network (NN) model can be described as a function $f : \mathcal{X} \to \mathcal{Y} \in [0,1]^c$ where c is the number of classes in the model. It is often composed of several layers of different types. A Multi Layer Perceptron (MLP) is a NN only composed of fully-connected layers: each neuron in one layer is connected to all neurons in the next layer, with a certain weight w (see Fig. 1). Multiclass Logistic Regressions (MLRs) are NNs that classify data into c different classes.

CNNs - often used in image classification - are NNs with mainly convolutional layers. These layers compute a convolution between *filters* F- 2-dimensional matrices smaller than the input of the layer - and the input of the layer. The elements of the filters are the weights of the layer. In most cases, a pooling layer, which performs a down-sampling of their input, follows convolutional layers (Scherer et al., 2010).

The weights are learnt through the optimization of a *loss function*. The most common one for CNNs is the categorical cross entropy (Srivastava et al., 2019). This optimization of a loss function is done over several runs - or *epochs* -, on a chosen dataset - the *training set*. This optimization problem is often solved using either Stochastic Gradient Descent (SGD) with Nesterov Momentum (Bengio et al., 2012) or Adam (Kingma and Ba, 2017), as they usually perform better than other optimizers.

2.2 Attack on Parameters

In 2016, Tramèr et al. (Tramèr et al., 2016) described several attacks on Machine Learning models. For neural networks, the authors described equation-solving and retraining attacks on small models. The retraining approaches required a much higher querying budget ($\times 20$) than the equation-solving attacks. In the context of CNNs, which have tens of thousands of parameters for small architectures, retraining attacks induce tremendous overhead. Thus, in what follows, we will only consider the equation-solving attack given the confidence values.

In Tramèr et al.'s equation-solving attack, the attacker knows the victim model's architecture, and can make as many queries to the model as necessary: their attacker randomly generates a set of query inputs, and receives the corresponding outputs. This provides them with a non-linear system of equations of the form:

$$f(x_i) = y_i \; \forall i \in \{1, ..., b\} \tag{1}$$

where b is the size of the generated input set.

The attacker then creates a new model with the same architecture as the victim model's and optimizes a categorical cross entropy loss function with the victim model's probability distribution - corresponding to the y_i queried beforehand - as the target distribution. This attack was successfully applied on MLRs and MLPs by Tramèr et al. In this paper, we try to protect CNNs against this attack on the last layer of the model.

2.3 Guided Grad-CAM

Not all neurons in a CNN have the same impact on predictions. Some works (Mahendran and Vedaldi, 2016) have asserted that the last layers of an image focus more on the global characteristics and tend to discard more details than the first ones. Thus, the analysis of the neurons used in those last convolutional layers might help determine the most relevant parts of an image for the NN's prediction.

The goal of visualization techniques such as saliency (K. Simonyan and Zisserman, 2014), Guided Backpropagation (J. T. Springenberg and Riedmiller, 2014) or Class Activation Maps (CAM) (Zhou et al., 2015) is to show the way the model makes its predictions. Indeed, given an image and a class label, they return a visualization of the parts of the image associated - according to the model - to the class label (see Fig. 3a and 3b in Sec. 4).

Guided Grad-CAM (Selvaraju et al., 2016) uses the gradients received at the last convolutional layer in order to compute such a visualization map. These gradients are closely related to the *importance weights* of the corresponding pixels. The importance weight of a pixel evaluates the impact a change in the pixel would have on the prediction. Guided Grad-CAM corresponds to a mix of Guided Backpropagation and a generalized version of CAM, Grad-CAM, and is resistant to adversarial attacks (Selvaraju et al., 2016): even though imperceptible noise is added to the image - leading to a wrong prediction -, the localization maps remain unchanged.

2.4 Related Works

Adding noise to the input of a model during the training phase is common practice. Indeed, it helps improve the accuracy and the generalizability of the model trained (An, 1996; Bishop, 1995). If no noise or regularization term is added, the training leads to an overfitting over the training data. Some papers also consider adding noise to the output of some layers or to the gradients during backpropagation to achieve a better accuracy and/or a faster convergence (Neelakantan et al., 2015; Audhkhasi et al., 2016). However, our defence does not consider the training phase: we only add noise during inference.

It is also interesting to note that noise injection can be used to defend against adversarial examples, and therefore to improve the NN's robustness. Gu and Rigazio add Gaussian noise and then use an autoencoder to remove it as a way of detecting adversarial examples (Gu and Rigazio, 2014).

Additive noise is also a common protection tool. Indeed, making a mechanism differentially private usually consists in adding noise to the output of the function to protect. This is, for instance, applied to the Stochastic Gradient Descent (SGD) during the training phase of a model to avoid leaking training data (Abadi et al., 2016). Since differential privacy provides security guarantees, Shokri and Shmatikov apply it to joint learning of NN models: their paper enables participants to jointly train a model by sharing the parameter updates with the other participants without leaking any information about their secret dataset (Shokri and Shmatikov, 2015).

However, our goal is different from the works mentioned above. Adding noise to the input has not been used to protect the parameters of a model. Moreover, visualization maps have not previously been applied to the selection of 'unimportant' pixels as suggested in this paper. In that sense, the method proposed here is believed to be original and introduces another use of saliency and visualization maps.

3 PROTECTING THE WEIGHTS: METHOD DESCRIPTION

This section details the threat model considered, as well as the method used to protect against the attack described in Sec. 2.2.

3.1 Threat Model

If no prior knowledge about the victim model - such as the architecture - is supposed, then an attacker trying to extract weights from a model needs to train several models from a - usually reduced - search space (Oh et al., 2018). Let us note that if the architecture is not known, it may be correctly guessed (Hong et al., 2018; Yan et al., 2018). Another option for such an attacker would be to conduct side-channel attacks, such as in (Batina et al., 2019). In our case, we will assume a stronger attacker, who already knows the architecture of the model. This is a plausible scenario given the various attacks on the architectures of CNNs (Batina et al., 2019; Yan et al., 2018; Hong et al., 2018).

Therefore, our threat model is the same as the one in Tramèr et al.'s paper (Tramèr et al., 2016):

- The attacker knows the architecture of the victim model.
- The attacker can query the victim model as many times as necessary. This means that the attacker can have at their disposal a set of pairs $(x, f(x))$ where x is in the input space, and $f(x)$ is its corresponding confidence values.

The goal of the attacker is to extract the parameters - here, essentially the weights - of a CNN. The original attack by Tramèr et al. extracted all of the model's parameters. However, we limited our study to the last layer of CNNs, due to their high number of parameters.

3.2 Adding Noise to the Input

The method proposed to protect the weights is to add random noise to the input image during the inference phase. Adding small amounts of noise can highlight the important features and improve the model's accuracy. On the other hand, adding too much noise leads to a drop in the victim model's accuracy. Thus, the challenge here is to add enough noise without altering the model's predictions.

With noisy inputs, the attacker gets a set of pairs $(x, f(x'))$ where $x' := x+n$ for some noise n unknown to the attacker, resulting in noisy extracted weights w' for the attacker.

The noise we will consider is a normal distribution over a selected set S of pixels, with either a high expected value - leading to a noisy output by linearity - or a high standard deviation. Batch normalization (BN) - a normalize layer - was introduced in 2015 by S. Ioffe and C. Szegedy to limit the change of distribution in the input during training, and therefore improve its speed, performance and stability (Ioffe and Szegedy, 2015). For each element $x_{i,j}$ in the input, the layer computes:

$$\widetilde{x}_{i,j} = \frac{x_{i,j} - \mu_{batch}}{\sqrt{\mathbb{V}_{batch} + \varepsilon}} \quad (2)$$

where μ_{batch} is the expected value of a given batch, $\mathbb{V}_{batch}$ is its variance and ε is a small positive value added in order to avoid division by 0.

Eq. 2 shows that the output of the BN layer is inversely proportional to the batch's standard deviation. Thus, adding noise with a high standard deviation decreases the dependence of the output with the original input values.

In order to add enough noise to alter the attacker's extracted weights without altering the victim model's predictions, we selected a set S of pixels considered to be "unimportant" to the model's predictions, and only added noise to those pixels. To do so, we computed the visualization map thanks to Guided Grad-CAM (Selvaraju et al., 2016) and set a threshold t. All neurons whose importance weights - in other words, whose value after Guided Grad-CAM was applied - are below t are selected to receive noise.

4 EXPERIMENTS

In this section, we detail the experiments carried on in order to select the set S of pixels we added noise to. We also explain the way the attack and defence were set up, and the results of the various experiments.

4.1 Selection of Pixels

Let us start this section by explaining the way we selected the pixels to modify in the input image using Grad-CAM.

The code used to run Guided Grad-CAM consists in a slight modification of the code found in (Gildenblat, 2017).

For clarity, let us consider the VGG19 architecture (Simonyan and Zisserman, 2014), for which Guided Grad-CAM performs well. Let *grad* denote the output image of the Guided Grad-CAM algorithm. Let t denote the threshold we choose to select the "unimportant indices". Let m be the maximum value in *grad*. Finally, let p denote the value of a pixel after Guided Grad-CAM was performed. Then, the selected pixels are such that $0 \leq p < t \times m$. For the VGG19 architecture, the noise we added to the selected pixels is a normal distribution with expected value $\mu = 125$ and standard deviation $\sigma = 25$.

(a) Image of a car from the CIFAR10 dataset

(b) Guided Grad-CAM

Figure 2: Visualization map resulting from Guided Grad-CAM applied to the image of a car from the CIFAR10 dataset, with the LeNet architecture.

The following paragraphs explain the way we set the threshold t.

Choosing $t = 0.25$ results in the images in Fig. 3. With the chosen threshold and noise, the model's predictions remain "African Elephant", with 1,038 pixels modified.

Since the predictions are unchanged, we can choose a higher threshold: $t = 0.42$ for instance, resulting in $5,820$ chosen pixels. The predictions remain intact, but the model is less certain about its predictions: the probability of the corresponding class ("African elephant"), lowers from 99.5% to, on average, 55.97%.

However, selecting the pixels close to half the maximal value - where the background pixels should be - results in mostly wrong predictions (around 97% of wrong predictions).

We give an example of a run of Guided Grad-CAM on five images in Fig. 4, with various thresholds. Table 1 summarizes the results depending on the threshold t chosen. Even though the impact of the noise varies greatly depending on the image, a threshold of $t = 0.25$ enables all predictions to remain correct, hence a choice of $t = 0.25$ to minimize the changes in the model's predictions.

Let us now consider the case of LeNet, the first CNN, introduced in 1998 by Lecun et al.(Y. LeCun and Haffner, 1998). Due to the limited depth of the architecture, guided Grad-CAM does not perform as well as on larger architectures such as VGG16 or VGG19 (Simonyan and Zisserman, 2014). However, it still outlines the important features of a class in the input image, as is shown in Fig. 2. In what follows, the "accuracy rate" will be defined as the per-

Table 1: Influence of the noise added with $\mu = 125$ and $\sigma = 25$ depending on the threshold t. The selected pixels have a value p in Guided Grad-CAM such that $0 \leq p < t \times \max(grad)$. The average class probability corresponds to the average probability associated to the correct class label over 100 trials.

Image	Threshold t	Number of pixels changed	Predictions unchanged	Initial class probability	Average class probability
African elephant	0.25	1,038	100%	99.48 %	98.92 %
	0.3	1,515	100%		95.53 %
	0.4	4,109	100%		95.28 %
	0.42	5,820	100%		57.01%
Coffee Mug	0.25	1,815	100%	89.09 %	59.79%
	0.3	2,491	85%		39.28 %
	0.4	5,593	0%		0 %
	0.42	7,546	0%		0 %
Monarch butterfly	0.25	1,905	100%	99.75 %	95.44 %
	0.3	4,726	100%		86.05 %
	0.4	7,894	100%		71.27 %
	0.42	10,440	86%		36.63 %
Dalmatian	0.25	1,198	100%	99.8 %	80.22 %
	0.3	1,496	100%		63.74 %
	0.4	2,623	0%		4.97 %
	0.42	2,222	0%		0 %
Egyptian cat	0.25	1,326	100%	42.29 %	58.66 %
	0.3	1,657	100%		43.35 %
	0.4	2,946	0%		0 %
	0.42	3,533	0%		0 %

(a) Original image

(b) Guided Grad-CAM (*grad*)

(c) Noisy image

(d) Noise added

Figure 3: Result of adding a noise with $\mu = 125$ and $\sigma = 25$ to the pixels whose value p in the Guided Grad-CAM map is such that $0 \leq p < t \times \max(grad)$ where $t = 0.25$.

centage of predictions that are equal to the victim model's original predictions. The noise added to the chosen pixels has an expected value of 0.8 (representing around 37.6% of the maximal value), and a standard deviation of 0.1 (representing around 4.7% of the maximum value). Similarly to the case of VGG19, we observed that a threshold of $t = 0.25$ resulted in unchanged predictions most of the time.

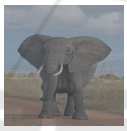

(a) African elephant[1]

(b) Coffee mug[2]

(c) Monarch butterfly[3]

(d) Dalmatian[4]

(e) Egyptian cat[5]

Figure 4: Images used for VGG19 predictions.

On the first 2,000 images of the CIFAR10 training set, this threshold leads, on average, to a modification of 2% of the pixels and an accuracy of 82%. This accuracy rate is above the one we get when we add noise to the whole image (around 79.8%). The drop in the accuracy rate can however be explained by LeNet's low prediction accuracy on CIFAR10 (the

[1]https://en.wikipedia.org/wiki/Elephant#/media/File:African Bush Elephant.jpg.

[2]https://github.com/Sanghyun-Hong/DeepRecon/tree/master/etc.

[3]https://www.4ritter.com/events-1/hummingbird butterfly-gardening.

[4]http://goodupic.pw/dog.html.

[5]https://www.pexels.com/photo/adorable-animal animal-photography-blur-259803/.

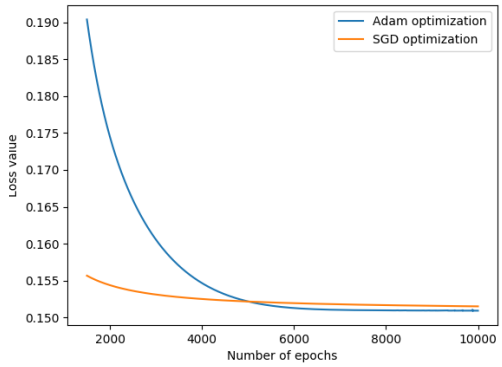

Figure 5: Last 8,500 epochs of SGD with Nesterov Momentum and Adam optimizersThe attack on weights is run on the the original LeNet architecture. We chose a budget query of 5,100 and ran the attack for 10,000 epochs.

model we trained had a 62% accuracy) and Guided Grad-CAM's reduced efficiency on LeNet. In Sec. 3.2, we also explained the influence of the noise on an architecture with a BN layer. Thus, we also studied a LeNet architecture where we added a BN layer after the first convolution. For this architecture, we kept the threshold of $t = 0.25$ and we switched the values of σ and μ: $\mu = 0.1$ and $\sigma = 0.8$. The accuracy of the model increased, as 89.5 % of the predictions were the same as the original model, yet only around 1.8 % of the pixels changed.

4.2 Attack on Weights

We applied Tramèr et al.'s attack on the last layer of a LeNet architecture, as well as a simplified LeNet architecture with only 6 filters instead of 16 in the first convolutional layer. The high accuracy rate Tramèr et al. reached on MLRs and MLPs only required 1,000 epochs (they extracted 2,225 parameters with a 99.8% accuracy for a query budget of $4,450$). Due to the large number of parameters in LeNet (62,006 for the original LeNet architecture), we focused our attack on the last dense layer. We show that the extraction of the weights can already be prevented if the attacker knows all the parameters except those in that last layer.

We chose Adam as an optimizer, since it provided a better accuracy on the extracted weights in the longer run, as can be seen in Fig. 5 .

Let us define the metric for the evaluation of the attack.

$$E(f,\widetilde{f}) = \sum_{x\in D} \frac{d(f(x),\widetilde{f}(x))}{|D|}$$
$$E_{var}(f,\widetilde{f}) = \sum_{x\in D} \frac{d_{var}(f(x),\widetilde{f}(x))}{|D|} \quad (3)$$

where f is the victim model, $\widetilde{f}$ is the extracted model and D is a test set.

The distance d is defined as follows: $d(x,y) = 0$ if $argmax(f(x)) = argmax(f(y))$ and $d(x,y) = 1$ otherwise. On the other hand, d_{var} is the total variation distance: $d_{var}(x,y) = \frac{1}{2}\sum_{i=0}^{c} |x_i - y_i|$ where c is the number of classes. For the dataset, we considered CIFAR10's testing set. The results of applying the attack on the LeNet architecture and its simplified version, with 30,000 epochs and a varying budget of queries can be found in Table 2.

Table 2: Adam Optimizations for the LeNet architecture where the second layer only has 6 filters, and for the original LeNet architecture. The attack was run on the last layer of the architecture, for 30,000 epochs.

Model	Unknowns	Number of parameters	Queries	$1-E$	$1-E_{var}$
Simplified LeNet Architecture	850	30,496	3,400	93.64 %	94.25 %
			4,250	95.77 %	96.43 %
			4,250	93.53 %	94.78 %
			5,100	95.87 %	96.33 %
LeNet Architecture	850	62,006	4,250 ($\alpha = 5$)	84.85 %	85.02 %
			5,100	81.34 %	81.37%
			5,950	84.37 %	84.29 %

We can observe that despite a lower accuracy than Tramèr et al.'s results, the extracted weights remain close to the original ones, with $1 - E > 80\%$ and $1 - E_{var} > 80\%$.

4.3 Efficiency of the Defence

Let us now run the attack on noisy images created thanks to Guided Grad-CAM. First, let us consider the original LeNet architecture with no BN layer. As explained in Sec. 3.2, we set $\mu = 0.8$ and $\sigma = 0.1$ for the noise's expected value and standard deviation, and we set $t = 0.25$ as the threshold on the output of Guided Grad-CAM. We also chose a query budget of $4,250$.

The attacker is given the model's architecture and its input, as well as the model's prediction for the noisy input. Fig. 6 shows the optimization of the weights when no noise was added to the input and when some noise was added. We ran the attack for 10,000 epochs, as the Adam optimizer almost reaches its optimum with this number of epochs.

Table 3: Evaluation of the extracted models on the original LeNet architectures and on the LeNet architecture with a BN layer - with and without noise. Their respective accuracy on the CIFAR10 testing dataset is 64.6% and 62.7%.

Model	Extraction Type	$1-E(f,\widetilde{f})$	$1-E_{var}(f,\widetilde{f})$	$\|\|w-\widetilde{w}\|\|$	Model Accuracy
LeNet	Not Noisy	77.36%	77.35%	5.90	58.15%
	Noisy	33.86%	33.81 %	24.25	30.34%
LeNet with Batch-Norm layer	Not Noisy	71.3%	73.8%	5.74	51.02%
	Noisy	56.9%	60.4 %	12.89	45.29%

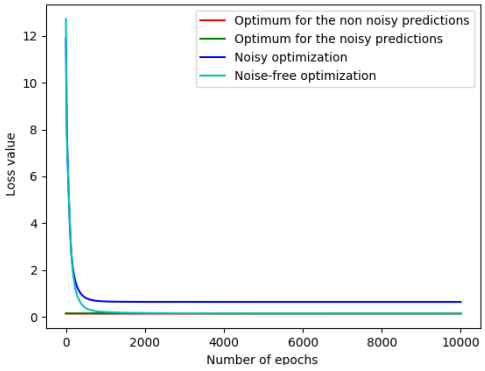

Figure 6: Attack on noisy images with a query budget of 5,100. The noise has an expected value $\mu = 0.8$ and a standard deviation $\sigma = 0.1$. The threshold on Guided Grad-CAM is $t = 0.25$.

Table 3 shows the evaluation of the defence on the LeNet architectures mentioned. In the case of the original LeNet, the noise dropped the extraction's accuracy from 77.36% to 33.86% with relation to E and from 77.35% to 33.81% with relation to E_{var}. The little noise added therefore resulted in a model whose predictions were far from the original model's predictions. A small change in some weights might induce a great difference in predictions, but we can check that this is not the case here. Let $w, \widetilde{w}$ and w' denote the targeted weights - from the last layer - of the victim model, the weights extracted from the non-noisy outputs and the ones extracted from the noisy outputs respectively. Then:

$$||w - \widetilde{w}|| = 5.90 \quad \text{and} \quad ||w - w'|| = 24.25 \qquad (4)$$

Thus, the weights extracted from the protected model are very different from the victim model's.

The fact that the attacker queries the model with inputs uniformly drawn might explain the efficiency of the defence. Indeed, the noise added keeps the predictions of the victim model close to the actual predictions when the input is drawn from the dataset, but it does not follow that the predictions will remain the same on random input. CNNs compute the probabilities of a certain input to be in each possible class. If the probabilities are low in each class, which is likely to happen with random input, any slight change in the input can lead to a change of prediction.

The results for the LeNet architecture with a BN layer can be seen in Table 3. In this case, we used 5,100 queries, $\mu = 0.1$, $\sigma = 0.8$ and $t = 0.25$, on 10,000 epochs. The difference between the model extracted from the noisy outputs and the non-noisy ones is not as clear as in the case without BN. However, the noise still impairs the extraction of the weights. Moreover, the advantage of this architecture is that the predictions remain close to the original model's predictions (the predictions are equal 89.5 % of the time, as mentioned in Sec. 4.1).

So far, we have only compared the extracted weights with the victim model's weights. However, the attacker can be satisfied if the extracted model has an accuracy rate on CIFAR10 that is equivalent or higher than the victim model's. Table 3 shows that this is not the case: the accuracy rate of the model extracted from noisy input is below both the victim model's and the model extracted without noise, in the considered cases.

5 CONCLUSION

This paper introduced a novel method to protect against Tramèr et al.'s equation-solving weight extraction attack using confidence values. Our method leads to noisier extracted weights for the attacker than the rounding of confidence values - as mentioned in Tramèr et al.'s paper -, with only a relatively small drop in the victim model's accuracy, which further work could aim at reducing. Moreover, our technique introduces a new use of visualization maps. We have described the way visualization maps - such as Guided Grad-CAM - can be used in order to select the less important pixels in an input image, and how to add noise to those selected pixels in order to protect the model's parameters.

Although Guided Grad-CAM generates overhead because of the computation of gradients, we have verified the efficiency of our defence on a LeNet architecture against an attack on the last layer's parameters.

However, this defence mechanism would not protect against side-channel attacks on CNNs (Duddu et al., 2018; Hong et al., 2018; Batina et al., 2019; Yan et al., 2018; Oh et al., 2018; Tramèr et al., 2016). Protecting the architecture and weights against these attacks could be the object of further study in the field.

Furthermore, in the equation-solving attack considered, the attacker generates random inputs in order to make as many queries as required. Our method relies on this randomness to protect the architecture's weights. Generating crafted inputs so as to prevent the added noise from interfering with the attack could be the object of further work.

Finally, as suggested by Tramèr et al., future work could focus on finding a way to apply differential privacy to protect the parameters rather than the input.

ACKNOWLEDGEMENTS

This work has been partially funded by the French ANR-17-CE39-0006 project BioQOP.

REFERENCES

Abadi, M., Chu, A., Goodfellow, I., McMahan, H. B., Mironov, I., Talwar, K., and Zhang, L. (2016). Deep learning with differential privacy. *Proceedings of the 2016 ACM SIGSAC Conference on Computer and Communications Security - CCS'16*.

Akhtar, N. and Mian, A. (2018). Threat of adversarial attacks on deep learning in computer vision: A survey. *arXiv preprint arXiv:1801.00553*.

An, G. (1996). The effects of adding noise during backpropagation training on a generalization performance. *Neural Computation*, 8(3):643–674.

Audhkhasi, K., Osoba, O., and Kosko, B. (2016). Noise-enhanced convolutional neural networks. *Neural Networks*, 78:15 – 23. Special Issue on "Neural Network Learning in Big Data".

Batina, L., Bhasin, S., Jap, D., and Picek, S. (2019). CSI NN: Reverse engineering of neural network architectures through electromagnetic side channel. In *28th USENIX Security Symposium (USENIX Security 19)*, pages 515–532, Santa Clara, CA. USENIX Association.

Bengio, Y., Boulanger-Lewandowski, N., and Pascanu, R. (2012). Advances in optimizing recurrent networks. *arXiv:1212.0901*.

Bishop, C. M. (1995). Training with noise is equivalent to tikhonov regularization. *Neural Computation*, 7(1):108–116.

Coskun, M., Uçar, A., Yildirim, Ö., and Demir, Y. (2017). Face recognition based on convolutional neural network,. *" International Conference on Modern Electrical and Energy Systems*, pages 376–379.

Deb, D., Zhang, J., and Jain, A. K. (2019). Advfaces: Adversarial face synthesis.

Dong, Y., Su, H., Wu, B., Li, Z., Liu, W., Zhang, T., and Zhu, J. (2019). Efficient decision-based black-box adversarial attacks on face recognition. *arXiv:1904.04433*.

Duddu, V., Samanta, D., Rao, D. V., and Balas, V. E. (2018). Stealing neural networks via timing side channels. *CoRR*, abs/1812.11720.

Gildenblat, J. (2017). Grad-cam implementation in keras.

Gu, S. and Rigazio, L. (2014). Towards deep neural network architectures robust to adversarial examples.

Hong, S., Davinroy, M., Kaya, Y., Locke, S. N., Rackow, I., Kulda, K., Sachman-Soled, S., and Dumitras, T. (2018). Security analysis of deep neural networks operating in the presence of cache side-channel attacks. *CoRR*, abs/1810.03487.

Inc., A. (2017). Face id security. white paper.

Ioffe, S. and Szegedy, C. (2015). Batch normalization: Accelerating deep network training by reducing internal covariate shift. *arXiv:1502.03167*.

J. T. Springenberg, A. Dosovitskiy, T. B. and Riedmiller, M. (2014). Striving for simplicity: The all convolutional net. *arXiv preprint arXiv:1412.6806*.

K. Simonyan, A. V. and Zisserman, A. (2014). Deep inside convolutional networks: Visualising image classification models and saliency maps. *CoRR*, abs/1412.6806.

Kingma, D. P. and Ba, J. L. (2017). Adam: A method for stochastic optimization. *arXiv:1412.6980*.

Krizhevsky, A., Sustskever, I., and Hinton, G. E. (2012). Imagenet classification with deep convolutional neural networks. *Advances in neural information processing systems*, pages 1097–1105.

Mahendran, A. and Vedaldi, A. (2016). Visualizing deep convolutional neural networks using natural preimages. *International Journal of Computer Vision*, pages 1–23.

Neelakantan, A., Vilnis, L., Le, Q. V., Sutskever, I., Kaiser, L., Kurach, K., and Martens, J. (2015). Adding gradient noise improves learning for very deep networks.

Oh, S. J., Augustin, M., Schiele, B., and Fritz, M. (2018). Towards reverse-engineering black-box neural networks. *International Conference on Learning Representations*.

Scherer, D., Müller, A., and Behnke, S. (2010). Evaluation of pooling operations in convolutional architectures for object recognition. pages 92–101.

Selvaraju, R. R., Das, A., Vedantam, R., Cogswell, M., Parikh, D., and Batra, D. (2016). Grad-cam: Visual explanations from deep networks via gradient-based localization. *CoRR*, abs/1610.02391.

Sharif, M., Bhagavatula, S., Bauer, L., and Reiter, M. K. (2016). Accessorize to a crime: Real and stealthy attacks on state-of-the-art face recognition. In *ACM Conference on Computer and Communications Security*.

Shokri, R. and Shmatikov, V. (2015). Privacy-preserving deep learning. In *Proceedings of the 22Nd ACM SIGSAC Conference on Computer and Communications Security*, CCS '15, pages 1310–1321, New York, NY, USA. ACM.

Simonyan, K. and Zisserman, A. (2014). Very deep convolutional networks for large-scale image recognition. *arXiv 1409.1556*.

Srivastava, Y., Murali, V., and Dubey, S. R. (2019). A performance comparison of loss functions for deep face recognition. *arXiv preprint arXiv:1901.05903*.

Tramèr, F., Zhang, F., Juels, A., Reiter, M. K., and Ristenpart, T. (2016). Stealing machine learning models via prediction apis. *USENIX Security*, pages 5–7.

Y. LeCun, L. Bottou, Y. B. and Haffner, P. (1998). Gradient-based learning applied to document recognition. *Proc. IEEE*.

Yan, M., Fletcher, C. W., and Torillas, J. (2018). Cache telepathy: Leveraging shared resource attacks to learn dnn architectures. *CoRR*, abs/1808.04761.

Zhou, B., Khosla, A., Lapedriza, A., Oliva, A., and Torralba, A. (2015). Learning deep features for discriminative localization.